

Discrimination of papillary renal cell carcinoma from benign proteinaceous cyst based on iodine and water content on rapid kV-switching dual-energy CT

İlkay Çamlıdağ 
Mehmet Selim Nural 
Cihan Kalkan
Murat Danacı 

PURPOSE

We aimed to evaluate whether rapid kV-switching dual energy CT (rsDECT) can discriminate between papillary renal cell carcinoma (RCC) and benign proteinaceous cysts (BPCs) based on iodine and water content.

METHODS

Twenty-four patients with histopathologically proven papillary RCC and 38 patients with 41 BPCs were retrospectively included. Patients with BPCs were eligible for inclusion when the cysts were stable in size and appearance for at least 2 years or proved to be a cyst on ultrasound or MRI. All patients underwent delayed phase (70–90 s) rsDECT. Iodine and water content of each lesion was measured on the workstation.

RESULTS

Of papillary RCC patients, 4 (16%) were female and 20 (84%) were male. Mean tumor size was 39 ± 20 mm. Mean iodine and water content was 2.08 ± 0.7 mg/mL and 1021 ± 14 mg/mL, respectively. Of BPC patients, 9 were female and 29 were male. Mean cyst size was 20 ± 7 mm. Mean iodine and water content was 0.82 ± 0.4 mg/mL and 1012 ± 14 mg/mL, respectively. There were significant differences between iodine and water contents of papillary RCCs and BPCs ($P < 0.001$). The best cutoff of iodine content for differentiating papillary RCC from BPC was 1.21 mg/mL (area under the curve [AUC]=0.97, $P < 0.001$, sensitivity 96%, specificity 88%, positive predictive value [PPV] 82%, negative predictive value [NPV] 97%, accuracy 91%); the best cutoff of water content was 1015.5 mg/mL (AUC=0.68, $P = 0.016$, sensitivity 83%, specificity 56%, PPV 52%, NPV 85%, accuracy 66%).

CONCLUSION

An iodine content threshold of 1.21 mg/mL accurately differentiates papillary RCC from BPCs on a single postcontrast rsDECT. Despite having a high sensitivity, water content has inferior diagnostic accuracy.

Any renal lesion with an attenuation of more than 20 Hounsfield units (HU) on postcontrast CT imaging is considered an indeterminate lesion and a second examination is generally necessary to determine whether the lesion is a benign proteinaceous cyst (BPC) or an enhancing tumor (1, 2). Differentiation between these lesions is very important as enhancing lesions require intervention, whether surgical or nonsurgical, if active surveillance option is not a consideration, while BPCs require no intervention or follow-up. Ultrasonography has shown to have high sensitivity and specificity classifying majority of these lesions as simple cysts (3); however, in case of a solid-appearing lesion on ultrasound, a dedicated renal mass characterization protocol CT or multiparametric MRI is still necessary for a definite diagnosis. This is time-consuming and results in increased patient anxiety, requires additional contrast material administration, and radiation dose is increased when CT is considered for imaging.

Incidental detection of renal lesions is on the rise, with lesions being detected in 13%–27% of cases undergoing abdominal imaging; more than half of renal cell carcinoma (RCC) cases are incidentally detected (4, 5). Hence, there is a growing need to characterize these high attenuation lesions as BPC or a tumor on a single contrast-enhanced CT imaging. In this regard, dual-energy CT (DECT) seems promising. DECT imaging is simultaneous acquisition

From the Departments of Radiology (İ.Ç. ✉ ilkayozaydin@hotmail.com, M.S.N., C.K.), and Urology (M.D.), Ondokuz Mayıs University School of Medicine, Samsun, Turkey.

Received 11 September 2019; revision requested 20 October 2019; last revision received 07 December 2019; accepted 24 December 2019.

Published online 23 July 2020.

DOI 10.5152/dir.2020.19483

You may cite this article as: Çamlıdağ İ, Nural MS, Kalkan C, Danacı M. Discrimination of papillary renal cell carcinoma from benign proteinaceous cyst based on iodine and water content on rapid kV-switching dual-energy CT. *Diagn Interv Radiol* 2020; 26:390–395

of a data set at two different energy spectra enabling decomposition of different materials based on their photoelectric absorption properties. Photoelectric absorption is the primary interaction way of X-rays with high atomic number materials and its occurrence is highly related with the energy of incident photon. As iodine has a much higher atomic number than the soft tissues of the body, it can be characterized and differentiated from soft tissues at high and low energy levels. Therefore, iodine is the most widely used and studied material in commercially available DECT systems and iodine quantification is another means of evaluation of enhancement within a tissue apart from the attenuation changes (6–8).

Out of six commercially available DECT systems, two are widely studied and provided more accurate results in terms of iodine quantification and monochromatic attenuation in a phantom study (9). High and low energy output is provided either by two different X-ray tubes on dual source DECT or a single X-ray tube that alternates between high and low energy on rapid kilovolt (kV)-switching DECT (rsDECT) in these systems. Spectral detector CT with two layers of detectors that separate low and high energy data, split-filter, sequential and slow kV-switching dual-energy scanning systems are also present albeit less available and studied (9, 10).

Studies regarding the differentiation of BPC from enhancing lesions based on iodine content has been studied before in both dual source (11–13) and rsDECT systems (7, 14–18). In a recent phantom study evaluating iodine quantification across different vendor systems and generations, all scanner types provided accurate iodine measurements although there was nonsignificant variability (9). However, *in vivo* studies with dual-source and rapid kV-switching

systems showed significant variability in iodine quantification thresholds such that a study performed with dual-source DECT (19) provided a threshold of 0.5 mg/mL for differentiating between enhancing and nonenhancing renal lesions whereas a threshold of 2 mg/mL was proposed in another study with rsDECT (7). Even in the rsDECT platform, there were various threshold values due to methodology differences.

In the majority of the studies performed with rsDECT (7, 16, 17, 20) enhancing lesions also included highly vascular lesions. On the other hand, in routine clinical practice, differentiation of a BPC from a highly vascular lesion is not quite problematic as attenuation difference between enhanced and unenhanced images is generally much more than 20 HU. The most problematic aspect is to differentiate BPC from papillary RCC which is quite hypovascular and sometimes does not even show any enhancement based on attenuation difference on CT (15, 21). In two studies that specifically evaluated the enhancement threshold between papillary RCC and BPC, Zarzour et al. (14), proposed a threshold of 1.28 mg/mL in nephrographic phase and Sadoughi et al. (18), a threshold of 1.20 mg/mL in corticomedullary phase. However, their sample sizes were small, with 12 papillary RCCs against 25 BPCs in the first study and 9 papillary RCC against 27 BPCs in the latter (14, 18). Therefore, their results require validation.

To our knowledge, there is no study investigating water content to differentiate a papillary RCC from BPC. Unlike dual source DECT, virtual unenhanced images provided by rsDECT is actually a water density image that provides water content in a region of interest (ROI) in mg/mL and attenuation information is obtained after postprocessing algorithms are applied (22). We hypothesized that water content in a BPC would be expected to be more than that of a solid papillary RCC and this could help differentiation between these lesions.

In this study, we aimed to investigate the best iodine and water content thresholds to differentiate papillary RCC from BPC.

Methods

This was a retrospective study approved by the institutional review board (IRB protocol number: 2019/205) and the requirement for informed consent from patients was waived.

Patient selection

Patients with BPCs and histopathologically proven papillary RCC who underwent abdominal rsDECT imaging between December 2015 and March 2019 were retrospectively evaluated.

Papillary RCC cases were histopathologically proven following laparoscopic partial nephrectomy and were included when they had preoperative unenhanced and contrast-enhanced DECT images. There were no exclusion criteria for this group of cases.

Inclusion criteria for BPCs were as follows: If the imaging was obtained in a renal mass characterization protocol that also contained unenhanced imaging, lesions with an attenuation between 20–70 HU on true unenhanced CT and showed less than 20 HU attenuation increase on postcontrast images were included. If the imaging was obtained as a single postcontrast CT examination for nonurinary complaints, lesions were eligible for inclusion when they had an attenuation of more than 20 HU on postcontrast CT. All cysts had to be stable in size and appearance for at least 2 years compared with previous CT examinations or have purely anechoic appearance on ultrasound, or be deemed as cyst on MRI. Cysts smaller than 10 mm craniocaudal diameter were excluded to eliminate the effect of partial volume averaging or pseudoenhancement.

Multidetector CT protocol

CT examinations were performed on a rapid kV-switching dual-energy 64-detector MDCT scanner (Discovery CT750 HD scanner, GE Healthcare). Unenhanced images covering the whole kidneys were obtained using a conventional 120 kVp single energy multidetector CT technique (scan type, helical; detector coverage, 40 mm; slice thickness, 5 mm; interval, 1.25 mm; pitch, 1.375:1; speed, 55; and gantry rotation time, 0.7 s). Postcontrast dual energy CT images were acquired in gemstone spectral imaging (GSI) mode of the abdomen at 70–90 seconds (s) after the contrast injection (scan type, helical; detector coverage, 40 mm; slice thickness, 2.5 mm; interval, 1.25 mm; pitch, 0.984:1; speed, 39.37; gantry rotation time, 0.7 s; automatic mA modulation range, 260–600 mA; targeted noise index, 17.25) which is the standard mode for majority of abdominal imaging indications in our institution. Images were reconstructed with a standard algorithm and application of 30% adaptive statistical iterative reconstruction (ASIR). The excretory

Main points

- On rsDECT, iodine content of 1.21 mg/mL can discriminate papillary renal cell carcinoma from benign proteinaceous cyst in a single postcontrast examination with very high accuracy.
- Water content threshold of 1015.5 mg/mL has poor diagnostic accuracy albeit having high sensitivity.
- A delayed postcontrast imaging at 70–90 s is more appropriate to evaluate enhancement of a high attenuation renal lesion based on the iodine content.

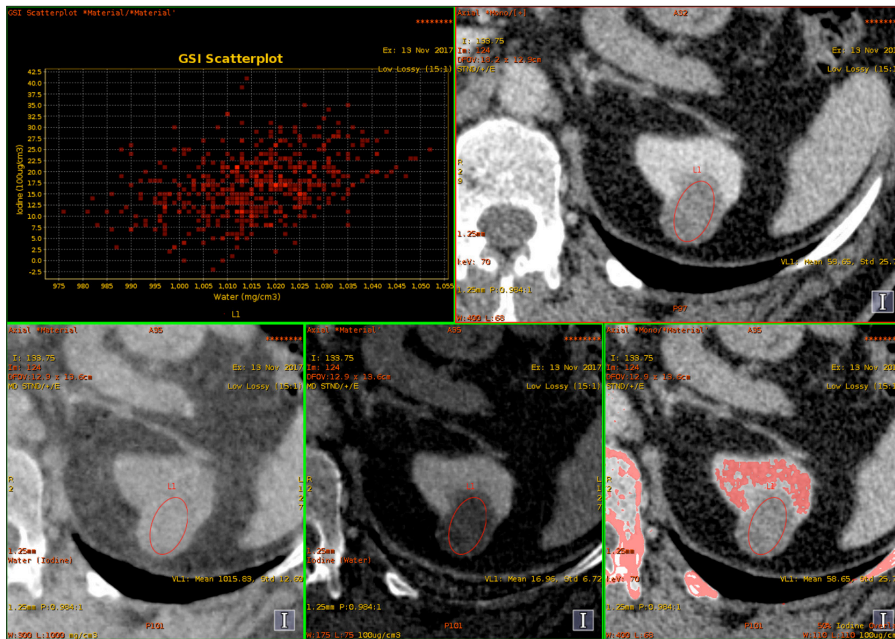


Figure 1. Material density analysis shows scatterplot depicting the iodine and water content of a papillary RCC case in the upper left panel. Nephrographic phase (90 s) 70 keV monochromatic image in the upper right panel shows the attenuation of the lesion (58 HU). Lower row panels from left to right show water density, iodine density, iodine overlay images, respectively. Water and iodine contents of the lesion were calculated as 1015 mg/mL and 1.69 mg/mL, respectively.

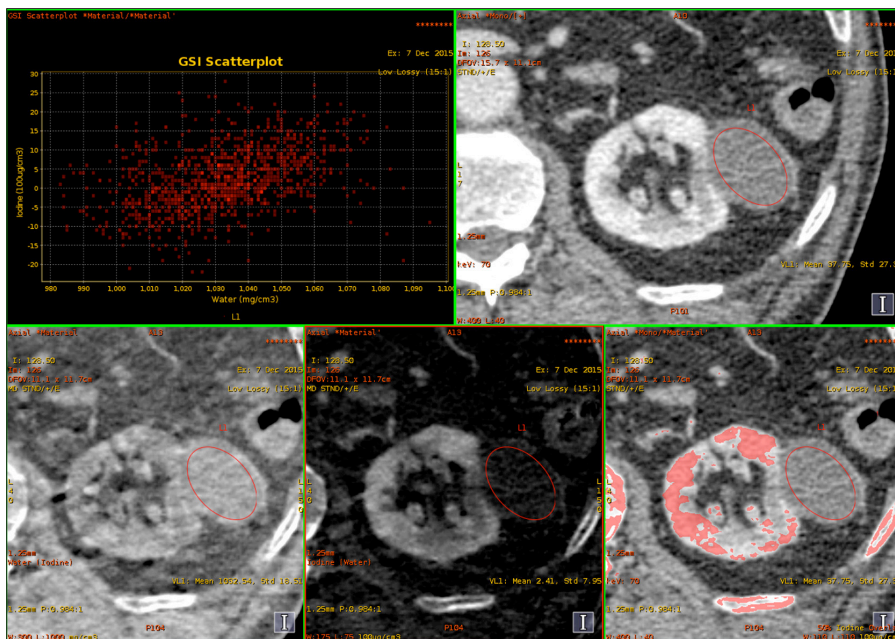


Figure 2. Material density analysis shows scatterplot depicting the iodine and water content of a BPC case in the upper left panel. Portal venous phase (70 s) 70 keV monochromatic image in the upper right panel shows the attenuation of the lesion (37 HU). Lower row panels from left to right show water density, iodine density, iodine overlay images, respectively. Water and iodine contents of the lesion were calculated as 1032 mg/mL and 0.24 mg/mL, respectively.

ry phase imaging, which is a component of our institution's standard protocol for renal lesion characterization, was acquired in single energy mode and with the same parameters to that of the unenhanced images except for the slice thickness, which is 2.5 mm

for the latter. However, these images were not used for analysis.

Intravenous contrast material was administered (Iohexol: Omnipaque 350, GE Healthcare) using a standardized weight-based dose injected at 2.5–4.0 cc/s rate for

a fixed 30 s injection interval, followed by a 25 cc normal saline bolus injected at the same rate as the contrast.

Image analysis

All image analyses were performed on a dedicated dual-energy workstation (ADW 2.0, GE Healthcare). Largest lesion size, attenuation value on true unenhanced images and delayed phase images were measured on axial images by a board-certified radiologist with 4 years of experience in abdominal radiology. For dual-energy material density image analysis, a second reader who was a second-year radiology resident was also involved to evaluate interrater reliability. Before the analyses, the experienced reader trained the radiology resident on how to place the regions of interests (ROIs) on 10 different cases who were not included in the study group. Then, both readers analyzed the lesions independently. ROIs were placed over the lesions on iodine density images to encompass homogeneous lesions as much as possible and the most intensely enhancing part of heterogeneous lesions and propagated between water density -70 keV monochromatic images to remain constant in size and location (Figs. 1, 2). The slice where the lesion was largest was chosen for homogeneous lesions, whereas the slice where the most intensely enhancing component was largest was chosen for heterogeneous lesions. Iodine and water content of each lesion were recorded in mg/mL. CT dose index volume (CTDIvol) of the delayed phase in dual-energy mode and single energy excretory phase were recorded in mGy.

Statistical analysis

Statistical analysis was carried out using SPSS 22.0 software package. Data were presented as mean±standard deviation (SD). Fisher's exact test was used to compare gender distribution across papillary RCC and BPC cases. Student t test was used for comparison between lesion size, attenuation, iodine and water content of papillary RCC and BPCs, and CTDIvol of single and dual energy acquisitions. Receiver operating characteristics (ROC) analysis was performed to evaluate the best cutoff of iodine and water content for differentiating papillary RCC from BPC. Youden index (J) was used to determine the best cutoff based on maximum sensitivity and specificity. To evaluate inter-

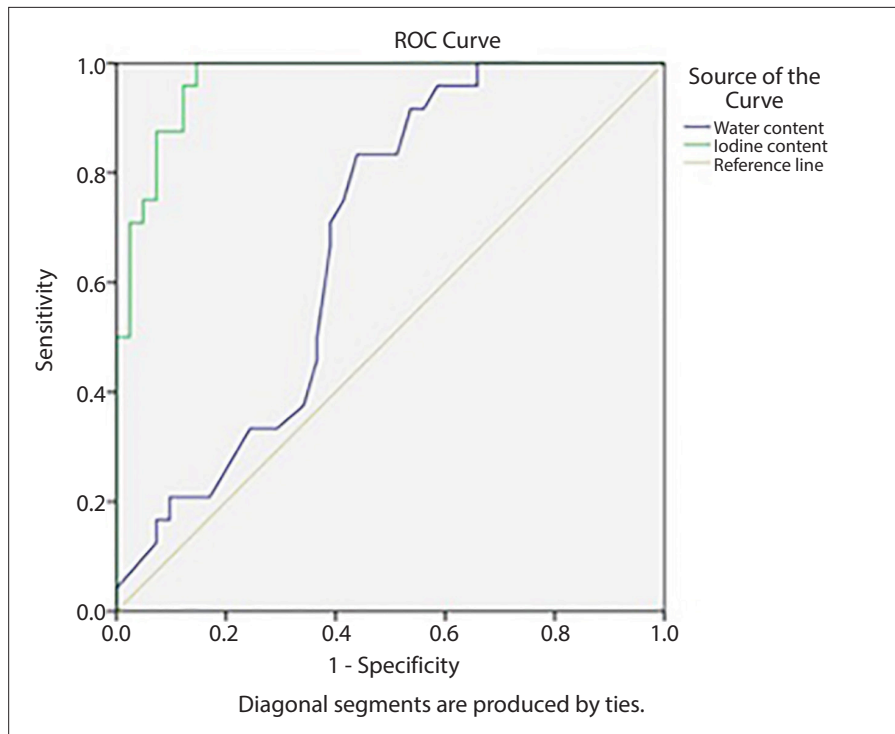


Figure 3. Receiver operating characteristic (ROC) curves for differentiating papillary RCC from BPC based on iodine and water content.

Table. Patient and tumor characteristics			
	Papillary RCC	BPC	P
Number of lesions (%)	24 (37)	41 (63)	
Gender (%)	20 M (84), 4 F (16)	29 M (76), 9 F (24)	0.45
Patient age (years), mean±SD	62±9	63±14	0.72
Lesion size (mm), mean±SD	39±20	20±7	<0.001
Unenhanced attenuation (HU), mean±SD	39±9	34±10	0.095
Mean nephrographic phase attenuation (HU), mean±SD	73±18	34±10	<0.001
Mean iodine content (mg/mL), mean±SD	2.08±0.7	0.82±0.4	<0.001
Mean water content (mg/mL), mean±SD	1021±7.8	1012±14	<0.001

RCC, renal cell carcinoma; BPC, benign proteinaceous cyst; M, male; F, female; HU, Hounsfield units; SD, standard deviation.

reader agreement for measuring iodine and water content, intraclass correlation coefficients and their 95% confidence intervals were calculated based on single measurement, absolute agreement, 2-way mixed model. Values less than 0.5 were indicative of poor reliability, values between 0.5 and 0.75 indicated moderate reliability, values between 0.75 and 0.9 indicated good reliability, and values greater than 0.90 indicated excellent reliability. The level of statistical significance was set as $P < 0.05$.

Results

Table demonstrates patient and tumor characteristics. There were 24 patients (37%) with papillary RCC and 38 patients (63%) with 41 BPCs. Patient age did not differ significantly between the two groups; male predominance was noted in both groups although it was not statistically significant ($P = 0.45$). There was significant size difference between papillary RCC lesions and BPCs (39±9 mm vs. 20±7 mm, $P < 0.001$).

There was no significant difference between mean unenhanced attenuation of

papillary RCC and BPCs (39±9 HU vs. 34±10 HU, $P = 0.095$) but the difference between postcontrast attenuation was significant (73±18 HU vs. 34±10 HU, $P < 0.001$). There was significant difference between mean iodine content of papillary RCC and BPCs (2.08±0.7 mg/mL vs. 0.82±0.4 mg/mL, $P < 0.001$). The best cutoff iodine content for differentiating papillary RCC from BPC was 1.21 mg/mL (area under the curve [AUC]=0.97, $P < 0.001$, sensitivity 96%, specificity 88%, positive predictive value [PPV] 82%, negative predictive value [NPV] 97%, accuracy 91%) (Fig. 3). Applying the iodine content threshold of 1.21 mg/mL, there was only one case of a false-negative papillary RCC with an iodine content of 1.18 mg/mL and 5 cases of false-positive BPC with iodine contents of 1.61, 1.49, 2.09, 1.3, 1.26 mg/mL, respectively.

There was also significant difference between mean water content of papillary RCC and BPCs (1021±7.8 mg/mL vs. 1012±14 mg/mL, $P = 0.001$). The best cutoff water content for differentiating papillary RCC from BPC was 1015.5 mg/mL (AUC=0.68, $P = 0.016$, sensitivity 83%, specificity 56%, PPV 52%, NPV 85%, accuracy 66%) (Fig. 3).

There was good agreement between two readers in iodine (ICC, 0.81; 95% CI, 0.70–0.88) and water content measurements (ICC, 0.88; 95% CI, 0.89–0.96) ($P < 0.001$).

The mean CT DIvol for dual-energy acquisitions were 17.46±6.6 mGy and 13.02±4.09 mGy for single-energy excretory phase imaging. The CT DIvol was significantly higher in dual-energy imaging ($P = 0.025$).

Discussion

In this study, we showed that iodine content on rsDECT can differentiate BPC from papillary RCCs with very good accuracy. On the other hand, the diagnostic power of water content was not as good as that of iodine despite having high sensitivity. It was noteworthy that papillary RCC, a solid tumor, had significantly higher water content than BPC (1021 mg/mL vs. 1012 mg/mL). Marin et al. (16) also found significantly higher water content in malignant renal lesions (1019 mg/mL), which consisted of clear cell, papillary and chromophobe RCC, than benign renal lesions (998 mg/mL), more than 90% of which consisted of simple cyst and BPC (16). Unfortunately, we do not have an explanation for why papillary RCC contained more water than BPC.

The first study in the literature to evaluate the threshold of enhancement with rsDECT was performed by Kaza et al. (7), who found an iodine content threshold of 2 mg/mL to differentiate enhancing renal lesions from nonenhancing lesions with high sensitivity and specificity. In this study, enhancing lesions were mainly oncocytoma, fat poor AML, histopathologically proven RCC, histologically unproven renal masses with increasing size, and Bosniak type III cysts. However, the number of enhancing lesions were low, consisted mainly of highly vascular lesions with substantial iodine content, and no subtype categorization was present. Meyer et al. (17) also investigated the threshold between 91 enhancing and 174 nonenhancing lesions very recently and suggested a threshold of 2 mg/mL for rsDECT system as well. However, similarly, they also included oncocytoma and other malignant tumor types apart from papillary RCC and hypervascular clear cell RCC was the most common tumor (n=58) in the enhancing lesions group. Marin et al. (16) proposed a threshold of 1.9 mg/mL in their study with a similar methodology. Patel et al. (20) found a threshold of 1.6 mg/mL in their study, in which enhancing lesions consisted of hyper and hypovascular renal masses; however, majority of the nonenhancing lesions consisted of simple cysts and this could have resulted in a lower threshold than those of the previously described studies. In a recently published study by Camlıdağ et al. (23), 95 histopathologically proven renal tumors were prospectively evaluated. In this study, it was shown that iodine content of clear cell RCC was much higher than that of papillary RCC (4.5 mg/mL vs. 2 mg/mL) and benign tumors had similar iodine content to that of clear cell RCC (3.3–3.4 mg/mL) (23). Given the difference in iodine content of various RCC subtypes and the lack of separate evaluation of each solid lesion subtype, we think that previously mentioned values might not be appropriate thresholds to differentiate papillary RCC and BPCs, since hypervascular lesions could have increased the threshold. Besides, in another very recent study by Sadooghi et al. (18), an iodine content threshold of 2 mg/mL did not have as good accuracy as when a threshold of 1.2 mg/mL were chosen for differentiating papillary RCC from BPCs. However, dual-energy image analyses were performed in corticomedullary phase in their study and cannot be applied to nephrographic phase. In the study

of Zarzour et al. (14), 12 papillary RCCs and 25 complex cysts were included, and iodine content threshold between cysts and papillary RCC were both evaluated in corticomedullary and nephrographic phases (14). The optimal threshold of iodine content for denoting enhancement was defined as 1.22 mg/mL in corticomedullary phase and 1.28 mg/mL in nephrographic phase. An iodine content threshold of 1.21 mg/mL in our study was quite in agreement with the other values that were proposed in previous studies with similar methodology (14, 18).

We think that a delayed phase (70–90 s) postcontrast examination is more suitable to evaluate iodine content of papillary RCC as these tumors progressively enhance (24) and attenuation values were found to be highly correlated with iodine content (23). Even in delayed phase, three papillary RCC patients in our study group showed indeterminate enhancement which was less than the threshold of 20 HU (15, 17 and 17 HU). Iodine contents of two of these cases (1.32 and 1.69 mg/mL) were above our threshold of 1.21 mg/mL. Moreover, there were more false negative cases of papillary RCC in the corticomedullary phase in the study by Zarzour et al. (14).

Our study had some limitations. First, the study design was retrospective and we had a small sample size. Second, histopathological diagnoses for BPCs were not present. Although we included BPCs showing at least 2 years of stability in size, it is well-known that BPCs can enlarge over time (25, 26) and interval size growth alone is also not an absolute criteria to raise the suspicion for malignancy unless accompanied by internal structural changes. However, BPCs in our study were also stable in appearance on follow-up imaging. Besides, regardless of the histopathological type, RCC can demonstrate minimal or no interval growth (27). Finally, due to the variability of thresholds across different DECT platforms, our current results could only be applicable to the rsDECT platform. Although iodine quantification was accurate across platforms with nonsignificant variability in a phantom study (9) and the difference in absolute iodine content was not found to be significant in an *in vivo* study (20), another study showed significantly higher values using rsDECT compared with dual-source DECT (17). These conflicting results limit the use of a material density threshold of one system for another. Patel et al. (20) suggested that normalization might have reduced

intermanufacturer variability. However, this topic needs validation with further studies in the future.

In conclusion, our results suggest that rsDECT can differentiate BPCs from papillary RCCs based on iodine content in a single postcontrast imaging with high accuracy, and additional imaging might not be needed in order to categorize high attenuation (>20 HU) renal lesions larger than 1 cm discovered on rsDECT.

Conflict of interest disclosure

The authors declared no conflicts of interest.

References

1. Israel GM, Bosniak MA. How I do it: evaluating renal masses. *Radiology* 2005; 236:441–450. [\[Crossref\]](#)
2. Jonisch AI, Rubinowitz AN, Mutalik PG, Israel GM. Can high-attenuation renal cysts be differentiated from renal cell carcinoma at unenhanced CT? *Radiology* 2007; 243:445–450. [\[Crossref\]](#)
3. Siddaiah M, Krishna S, McInnes MDF, et al. Is Ultrasound Useful for Further Evaluation of Homogeneously Hyperattenuating Renal Lesions Detected on CT? *AJR Am J Roentgenol* 2017; 209:604–610. [\[Crossref\]](#)
4. Gill IS, Aron M, Gervais DA, Jewett MA. Clinical practice. Small renal mass. *N Engl J Med* 2010; 362:624–634. [\[Crossref\]](#)
5. Lindblad P. Epidemiology of renal cell carcinoma. *Scand J Surg* 2004; 93:88–96. [\[Crossref\]](#)
6. Agrawal MD, Pinho DF, Kulkarni NM, Hahn PF, Guimaraes AR, Sahani DV. Oncologic applications of dual-energy CT in the abdomen. *Radiographics* 2014; 34:589–612. [\[Crossref\]](#)
7. Kaza RK, Caoili EM, Cohan RH, Platt JF. Distinguishing enhancing from nonenhancing renal lesions with fast kilovoltage-switching dual-energy CT. *AJR Am J Roentgenol* 2011; 197:1375–1381. [\[Crossref\]](#)
8. Marin D, Boll DT, Mileto A, Nelson RC. State of the art: dual-energy CT of the abdomen. *Radiology* 2014; 271:327–342. [\[Crossref\]](#)
9. Jacobsen MC, Schellingerhout D, Wood CA, et al. Intermanufacturer comparison of dual-energy CT iodine quantification and monochromatic attenuation: a phantom study. *Radiology* 2017; 170896.
10. McCollough CH, Leng S, Yu L, Fletcher JG. Dual-and multi-energy CT: principles, technical approaches, and clinical applications. *Radiology* 2015; 276:637–653. [\[Crossref\]](#)
11. Ascenti G, Mazziotti S, Mileto A, et al. Dual-source dual-energy CT evaluation of complex cystic renal masses. *AJR Am J Roentgenol* 2012; 199:1026–1034. [\[Crossref\]](#)
12. Chandarana H, Megibow AJ, Cohen BA, et al. Iodine quantification with dual-energy CT: phantom study and preliminary experience with renal masses. *AJR Am J Roentgenol* 2011; 196:W693–700. [\[Crossref\]](#)
13. Mileto A, Marin D, Ramirez-Giraldo JC, et al. Accuracy of contrast-enhanced dual-energy MDCT for the assessment of iodine uptake in renal lesions. *AJR Am J Roentgenol* 2014; 202:W466–474. [\[Crossref\]](#)

14. Zarzour JG, Milner D, Valentin R, et al. Quantitative iodine content threshold for discrimination of renal cell carcinomas using rapid kV-switching dual-energy CT. *Abdom Radiol* 2017; 42:727–734. [\[Crossref\]](#)
15. Couvidat C, Eiss D, Verkarre V, et al. Renal papillary carcinoma: CT and MRI features. *Diagn Interv Imaging* 2014; 95:1055–1063. [\[Crossref\]](#)
16. Marin D, Davis D, Roy Choudhury K, et al. Characterization of small focal renal lesions: diagnostic accuracy with single-phase contrast-enhanced dual-energy CT with material attenuation analysis compared with conventional attenuation measurements. *Radiology* 2017; 284:737–747. [\[Crossref\]](#)
17. Meyer M, Nelson RC, Vernuccio F, et al. Comparison of iodine quantification and conventional attenuation measurements for differentiating small, truly enhancing renal masses from high-attenuation nonenhancing renal lesions with dual-energy CT. *AJR Am J Roentgenol* 2019;W1–11. [\[Crossref\]](#)
18. Sadoughi N, Krishna S, Macdonald DB, et al. Diagnostic accuracy of attenuation difference and iodine concentration thresholds at rapid-kilovoltage-switching dual-energy CT for detection of enhancement in renal masses. *AJR Am J Roentgenol* 2019; 213:619–625. [\[Crossref\]](#)
19. Mileto A, Marin D, Alfaro-Cordoba M, et al. Iodine quantification to distinguish clear cell from papillary renal cell carcinoma at dual-energy multidetector CT: a multireader diagnostic performance study. *Radiology* 2014; 273:813–820. [\[Crossref\]](#)
20. Patel BN, Vernuccio F, Meyer M, et al. Dual-energy CT material density iodine quantification for distinguishing vascular from nonvascular renal lesions: normalization reduces intermanufacturer threshold variability. *AJR Am J Roentgenol* 2019; 212:366–376. [\[Crossref\]](#)
21. Vikram R, Ng CS, Tamboli P, et al. Papillary renal cell carcinoma: radiologic-pathologic correlation and spectrum of disease. *Radiographics* 2009; 29:741–757. [\[Crossref\]](#)
22. Morgan DE. Dual-energy CT of the abdomen. *Abdom Imaging* 2014; 39:108–134. [\[Crossref\]](#)
23. Camlidag I, Nural MS, Danaci M, Ozden E. Usefulness of rapid kV-switching dual energy CT in renal tumor characterization. *Abdom Radiol* 2019; 44:1841–1849. [\[Crossref\]](#)
24. Kim JK, Kim TK, Ahn HJ, Kim CS, Kim KR, Cho KS. Differentiation of subtypes of renal cell carcinoma on helical CT scans. *AJR Am J Roentgenol* 2002; 178:1499–1506. [\[Crossref\]](#)
25. Gabr AH, Gdor Y, Roberts WW, Wolf JS Jr. Radiographic surveillance of minimally and moderately complex renal cysts. *BJU Int* 2009; 103:1116–1119. [\[Crossref\]](#)
26. Israel GM, Bosniak MA. Follow-up CT of moderately complex cystic lesions of the kidney (Bosniak category IIF). *AJR Am J Roentgenol* 2003; 181:627–633. [\[Crossref\]](#)
27. Kunkle DA, Crispin PL, Chen DY, Greenberg RE, Uzzo RG. Enhancing renal masses with zero net growth during active surveillance. *J Urol* 2007; 177:849–854. [\[Crossref\]](#)